EurJIC
European Journal of Inorganic Chemistry

Research Article
doi.org/10.1002/ejic.202200245

Chemistry Europe
European Chemical Societies Publishing

www.eurjic.org

Superoxide Reduction by Cu-Amyloid Beta Peptide Complexes: A Density Functional Theory Study

Federica Arrigoni,[a] Chiara Di Carlo,[a] Alberto Rovetta,[a] Luca De Gioia,[a] Giuseppe Zampella,[a] and Luca Bertini*[a]

Oxidative stress and copper dyshomeostasis are well established factors in the course of Alzheimer's disease (AD). Indeed, the pathological interaction of copper with the amyloid peptide is able to induce reactive oxygen species (ROS) production through a three-step cycle in which O_2 is gradually reduced to superoxide, oxygen peroxide and finally to highly neurotoxic $OH^{\bullet}$ radicals. The purpose of this study has been to investigate at a computational level, by Density Functional Theory (DFT) and molecular mechanics techniques, the final two steps of O_2 reduction to $OH^- + OH$ radical i.e the superoxide and hydroperoxide reduction by ascorbate, on different Cu(II)·Aβ coordination models. At variance with the first step of O_2 reduction to $O_2^{\bullet-}$ characterized by high energy barrier, the successive $O_2^{\bullet-}$ and O_2H^- reductions are low energy barriers processes and that the $OH^{\bullet}$ radical formation is further favored by the possibility of Cu(II)·Aβ to form the Asp1 amino terminal radical. We discuss the results obtained from the perspective of the recent findings in the Aβ redox chemistry in AD pathology.

Introduction

Alzheimer's disease (AD) is the most common and prevalent cause of dementia in the elderly.[1–3] The most recent report by the GBD 2019 Dementia Forecasting collaborators[4] estimates that the number of people with dementia worldwide in 2019 (57 million) would almost triple in 2050 (153 million).

The amyloid hypothesis has been the guide of scientific research and the model for the pathogenesis of AD.[5–7] Aβ peptides are released from neuronal transmembrane Amyloid Precursor Protein (APP) by the sequential protease activity and possess the ability aggregate into many different conformations from soluble small Aβ oligomers to insoluble fibrils, which are the primary component of the senile plaques actually observed in AD patients. Among these, small oligomers rather than the monomers or insoluble fibrils are considered neurotoxic[8,9] inducing AD neuropathology. In the context of the amyloid hypothesis the formation of tau-dependent neurofibrillary tangles aggregation occurs downstream of Aβ aggregation.

More recently oxidative stress associated with transition metal dyshomeostasis became a significant issue in understanding the pathogenesis of AD.[6–10] Oxidative stress is a condition that arises when ROS production exceeds biochemical means of scavenging these species, and is manifested, among other ways, by protein oxidation[17–20] and lipid peroxidation.[21,22,23] Transition metal mislocalization, accumulation and dyshomeostasis can drive pathological changes in brain and other tissues.

The scientific community involved in AD research agrees that there is a clear link between oxidative stress and transition metal dyshomeostasis.[13,16,24,25] When bound to Aβ peptide, Cu(II)Aβ is redox active and keeps the propensity to produce ROS in vitro although to a lesser extent compared to Cu(II) in solution.[11,26] Here there is the link between copper dyshomeostasis, oxidative stress and amyloid cascade hypothesis: Aβ peptides possess the ability to bind Cu(II)[27,28] which are able to promote and modulate Aβ aggregation[29] to Aβ oligomers of which are considered the *Optimal Generators*[30] of reactive oxygen species (ROS) and as upstream pathogenic drivers in AD. Finally, these Cu(II)Aβ oligomers aggregate on a longer time scale inducing copper recruitment in the amyloid plaque in the millimolar range.[31–33]

Since the first clinical evidence of the copper dyshomeostasis and oxidative stress in post-mortem AD brains samples,[31,34–37] the continuous research of the redox chemistry of copper and Aβ peptide allowed to delineate a further hypothesis alongside with the "classic" amyloid cascade hypothesis in the etiology of AD.

It is well-recognized that the Cu(II)-Aβ species is redox active and is a potential direct source of ROS in the presence of molecular oxygen and a reducing agent such ascorbate.[26,38] O_2 reduction mechanism depicted in Figure 1 has been intensively investigated since it is fundamental in the understanding of the oxidative stress in AD.

In presence of a reducing agent such as Ascorbate ($AscOH^-$)[41] that is abundant in brain, O_2 is gradually reduced to hydroxyl anion and hydroxyl radical conveying the ascorbate electrons through Cu(II)·Aβ/Cu(I)·Aβ cycling.

[a] *Dr. F. Arrigoni, Dr. C. Di Carlo, Dr. A. Rovetta, Prof. L. De Gioia, Prof. G. Zampella, Prof. L. Bertini*
Department of Biotechnologies and Biosciences,
University of Milano-Bicocca,
Piazza della Scienza 2, 20126 Milan, Italy
E-mail: luca.bertini@unimib.it

Supporting information for this article is available on the WWW under https://doi.org/10.1002/ejic.202200245

Part of the Chemistry Europe joint Special Collection on Quantum Bioinorganic Chemistry.

Research Article
doi.org/10.1002/ejic.202200245

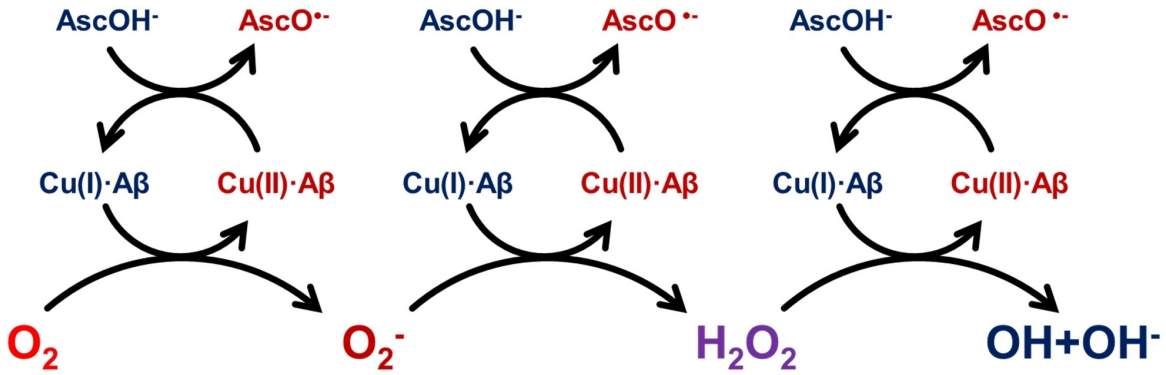

Figure 1. The $OH^{\bullet}$ radical production process catalyzed by Cu(II)·Aβ in presence of ascorbate as a one-electron reductant agent. The redox Fenton-like cycling of Cu(II)·Aβ/Cu(I)·Aβ in aerobic conditions results in the production of $O_2^{\bullet-}$, H_2O_2 and the hydroxyl radical plus OH^-.The process starts with the population of the so-called "*in-between-state*" Cu(II)·Aβ species, characterized by a lower copper coordination number[39] that can bind ascorbate and undergoes reduction. Cu(I)·Aβ can bind and reduce molecular oxygen to superoxide. This latter is considered the slow step of the process.[40] The same cycling can reduce superoxide to hydrogen peroxide and finally to $OH^{\bullet}$ radical plus OH^-.

The process starts with the 3N2O Cu(II)·Aβ component I coordination which is predominant at physiological pH and involves Asp1 N-terminal amine and carboxylate side chain, the Asp1–Ala2 carbonyl group and two imidazole rings from from His6 and His13/His14.[42–46] Upon population of an higher energy 3 N1O intermediate coordination, the reduction Cu(II)·Aβ to Cu(I)·Aβ by $AscOH^-$[39,47] occurs with the formation of a three-coordinated Cu(I)·Aβ species[48,49] which can bind O_2. This latter step is considered the rate-determining step of the whole process and Cu(I)·Aβ·O_2 is reduced to Cu(I)·Aβ·$O_2^{\bullet-}$ as experimentally shown by Reybier et al.[50] and confirmed by this lab using quantum chemistry techniques.[40]

$O_2^{\bullet-} \rightarrow H_2O_2$ and $H_2O_2 \rightarrow OH^{\bullet} + OH^-$ steps are similar: the adduct Cu(II)·Aβ·substrate binds $AscOH^-$, reducing the substrate and releasing $AscO^{\bullet-}$ radical. According to recent experimental and computational[26,40] investigations, the redox competent coordination for ROS generation involves three ligands from the Aβ peptide, i.e at least one His side chain plus Asp1 N-terminal and/or carboxylate and/or a second His side chain. During ROS generation this coordination is populated allowing substrate and $AscOH^-$ binding to the metal center.

Despite the enormous efforts made by the scientific community to investigate transition metal dyshomeostasis and oxidative stress in AD, studies conducted to date did not prove a clear beneficial effect of antioxidant treatment in AD patients.[51–53] In this context it is clear that further efforts to investigate these mechanisms at molecular level are welcome to developing new therapeutic strategies. Moreover it is taking shape the idea that copper bound Aβ to could either be a sensor for various imaging in AD diagnosis[54–56] or a pharmacological target for a chetaling or redox therapeutic strategy in AD.[55,57,58]

The experimental characterization of the different chemical species involved in ROS production is difficult since their transient nature, but computational approaches can overcome these difficulties.[59,60,61] In this paper we focus on the second and third steps of ROS generation in which $O_2^{\bullet-}$ is reduced to H_2O_2, and finally to $OH^{\bullet} + OH^-$ applying Density Functional Theory (DFT) approach starting from the redox competent coordinations of the Cu(II)·Aβ superoxide adduct[40] and considering the explicit presence of ascorbate as reductant.[62,63]

Computational Details

The DFT computations were performed using the pure GGA BP86[64,65] DFT functional and RI technique[66] as implemented in TURBOMOLE.[67] Basis sets of triple-ζ plus polarization split valence quality[68] were adopted for all atoms. Solvent effect is accounted for by using the COSMO (Conductor-like Screening Model) approach.[69] Water solvation has been considered by setting the dielectric constant equal to 80. This computational setting provides ground state geometry parameters in good agreement with experimental X-ray values.[49,70] Charge distribution was evaluated using Natural bond orbital analysis (NBO). Ground state geometry optimizations were carried out with convergence criteria fixed to 10^{-6} hartree for the energy and 0.001 hartree bohr^{-1} for the gradient norm vector. In the framework of the single-determinant DFT approach, the antiferromagnetic coupling of the Fe atoms in the C-cluster has been treated within the spin-unrestricted broken-symmetry formalism (BS).[71] In Table S1a in SI are reported the $< S^2 >$ obtained for the main coordinations investigated in this paper. The effects of ZPE, thermal and entropic contributions on the purely electronic total energy values to compute free energies have been investigated by means of evaluation of the approximated roto-translational partition function of each molecular species, at T = 298 K and P = 1 bar using FREEH script.

Results

Superoxide reduction

The process of H_2O_2 production from O_2^- assisted by Cu(II)·Aβ in presence of ascorbate as an electron source can be described as in Scheme 1.

Research Article
doi.org/10.1002/ejic.202200245

Chemistry Europe
European Chemical Societies Publishing

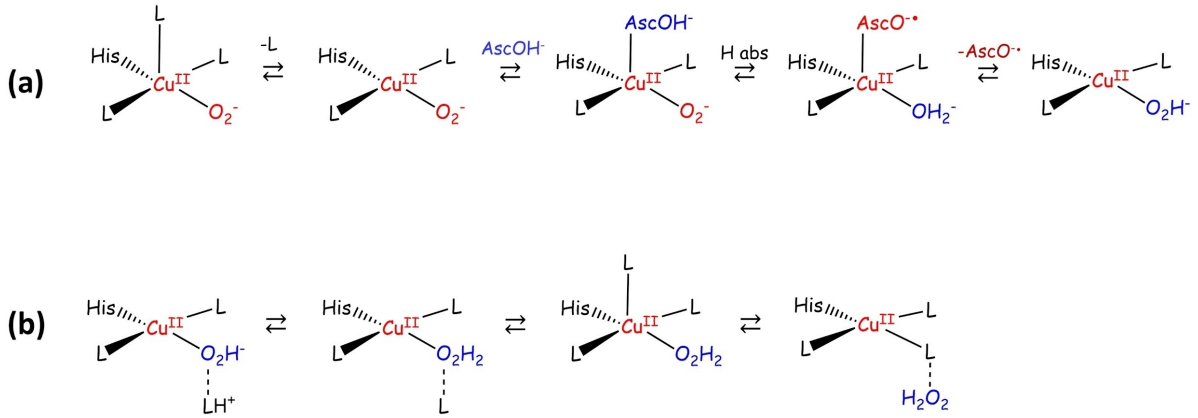

Scheme 1. Superoxide reduction pathway catalyzed by Cu(II)·Aβ with Ascorbate as a reductant species. In (a) the pathway from the Cu(II)·Aβ·$O_2^{\bullet-}$ to Cu(II)·Aβ·O_2H^- systems is described. In (b) the latter is involved in the protonation of the O_2H^- hydroperoxide ligand until the H_2O_2 release.

The Cu(II)·Aβ·$O_2^{\bullet-}$ system is the product of the previous $^3O_2$ reduction, as described in ref.[40] and has a four- or five-coordinated metal center. The next step is the binding of the $AscOH^-$ ascorbate ion with the formation of the five coordinated Cu(II)·Aβ·$O_2^{\bullet-}$·$AscOH^-$, which successively undergoes hydrogen atom abstraction resulting in the reduction of the superoxide to hydroperoxide ion[72,73,74] and in the formation of the $AscO^{\bullet-}$ ascorbyl radical. After the dissociation of the $AscO^{\bullet-}$, the four coordinated Cu(II)·Aβ·O_2H^- will be in equilibrium.

1. with its protonated form Cu(II)·Aβ·O_2H_2;
2. with a Cu(II)·Aβ four coordinated form releasing the H_2O_2.

In the following sections we analyze each step of this process considering the possible Cu(II)·Aβ·$O_2^{\bullet-}$ redox competent coordinations proposed on the basis of previous experiments[26] and computations.[40] Table S1 in SI report the shape and the main geometry parameters for the various forms investigated in this investigation.

Stability of the Cu(II)·Aβ·O_2^- coordination modes

In this section we describe Cu(II)·Aβ·$O_2^{\bullet-}$ structures with a coordination number CN ≤ 5 that comes from the O_2 reduction step as sketched in Scheme 2.

We consider a) three four-coordinated models (the mono-histidine form **1** and the two bis-histidine model **2** and **3**, Scheme 2A); b) four and pentacoordinated bis-histidine forms (mono-histidine form **1a** derived from **1** in which one extra imidazole ring form an hydrogen bond interaction with the amino terminal; pentacoordinated **2a** form in which both Asp1 amino terminal and carboxylate side chain are coordinated to Cu(II), Scheme 2B).

Introducing **1a** and **2a** models, mono-histidine and bis-histidine models are structural isomers and their energies can be compared.

Cu(II)·Aβ·$O_2^{\bullet-}$ structures have an end-on Cu(II)-superoxide motif with a triplet ground state, while singlet solution results higher in energy and broken symmetry (BS) singlet solution collapses on this latter. The models in Scheme 2 are all very close in energy, being the pentacoordinated **2a** the most stable, although **1a** and **3** are only 1.8 and 2.3 kcal/mol higher in energy.

The metal ions are reduced on average by 0.3 e so that the actual oxidation state of Cu is 1.6. Compared to free $O_2^{\bullet-}$, the O–O distance in Cu(II)·Aβ·$O_2^{\bullet-}$ is on average 0.082 Å shorter with a larger spin population on average by 0.4 e, indicating the partial charge transfer from to O_2^- to Cu. This result indicates that Cu is partially reduced by O_2^-, in line with the negative reduction potential of the O_2/O_2^- couple of −0.18 V (See SI Figure S1 and S2 and ref [40] for details)

We evaluate the propensity of **1** Cu(II)·Aβ·$O_2^{\bullet-}$ model to release $O_2^{\bullet-}$ in solution as suggested by the Rabyer et at.[50] computing the energy difference of the following process, equation (1):

$$\mathrm{Cu(II)\cdot A\beta\cdot O_2^{\bullet-} + R\cdot H_2O \rightleftharpoons Cu(II)\cdot A\beta\cdot H_2O + R\cdot O_2^{\bullet-}} \quad (1)$$

where i) Cu(II)·Aβ·H_2O is the component1 coordination[42,43] (see SI Figure 2B) with one His side chain and one apical water molecule; ii) R·H_2O and R·$O_2^{\bullet-}$ are the water and superoxide adducts with positively charged Arginine side chain, respectively.

The choice of the Arg side chain has been made to stabilize as much as possible the free $O_2^{\bullet-}$ ion in solution. We also recall that Arg5 is actually a residue that is in principle close to the Cu(II) coordination sphere. The energy difference according to equation (1) is 5.3 kcal/mol, suggesting that $O_2^{\bullet-}$ ion can leave the Cu(II) coordination sphere when its negative charge is sufficiently stabilized.

First step: ascorbate binding

Because the highest Cu(II) coordination number is 5, we conclude that in Cu(II)·Aβ·$O_2^{\bullet-}$·$AscOH^-$ at least one ligand must be dissociated to accommodate the ascorbate (see

Research Article
doi.org/10.1002/ejic.202200245

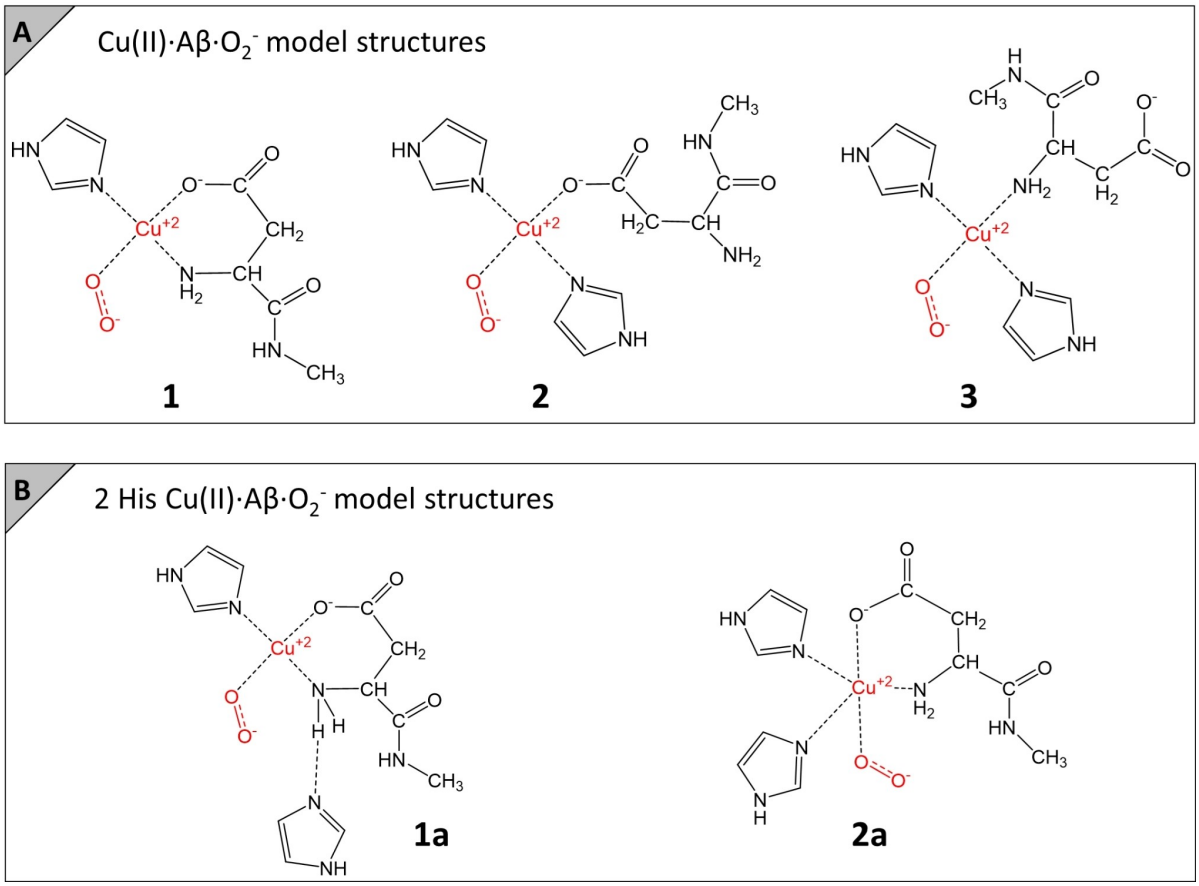

Scheme 2. Mono- and bis-histidine Cu(II)·Aβ·$O_2^{\bullet-}$ models considered in this paper. Model **1 a** has one imidazole ring that forms an hydrogen bond interaction with the amino terminal thus allowing the evaluation of its stability with respect to those of models **2**, **3** and bis-histidine model **2 a**.

Scheme 1a). The four Cu(II)·Aβ·$O_2^{\bullet-}$ structures are in an energy range of 3.2 kcal/mol and therefore in principle all can equally contribute to this reactivity.

In the search of the Cu(II)·Aβ·$O_2^{\bullet-}$·$AscOH^-$ minimum form we select the structures in which the free hydroxyl group that belong enediol group of the ascorbate form an H-bonding interaction with the superoxide

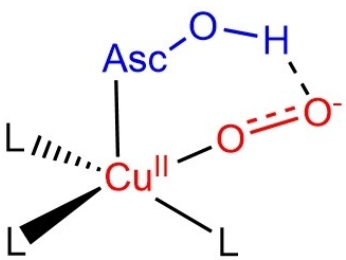

which will be the starting point for the e^-/H^+ transfer during the redox process.

The Asc(OH)$^-$ adducts have a triplet ground state with trigonal-bipyramidal geometry. The spin population is almost completely localized on Cu(II) and the superoxide, with an oxidation state of Cu equal to 1.7.

The $AscOH^-$ affinity is low due to the partial reduction of the metal center. We evaluate the $AscOH^-$ binding energy according to the equilibrium 2a and 2b

$$\mathrm{Cu(II)\cdot A\beta\cdot O_2^{\bullet-} + AscOH^- \rightleftharpoons Cu(II)\cdot A\beta\cdot O_2^{\bullet-}\cdot AscOH^-} \quad (2a)$$

$$\mathrm{Cu(II)\cdot A\beta\cdot O_2^{\bullet-}\cdot (H_2O) + AscOH^- \rightleftharpoons Cu(II)\cdot A\beta\cdot O_2^{\bullet-}\cdot AscOH^- + H_2O} \quad (2b)$$

where in 2b ascorbate binding is described as the replacement of a water molecule by $AscOH^-$. According to equation (2a) and equation (2b), $AscOH^-$ binding free energy is on average only −1.5 kcal/mol and −1.2 kcal/mol, respectively. We compare this latter value with the ascorbate binding to Cu(II)·Aβ model coordination, equal to −10.2 kcal/mol.[40] The decreasing of the ascorbate affinity going from Cu(II)·Aβ to Cu(II)·Aβ·$O_2^{\bullet-}$ can be attributed to the partial Cu(II) reduction in the superoxide moieties, as clearly evidenced by the higher copper spin population in Cu(II)·Aβ (0.21 e on average).

Research Article
doi.org/10.1002/ejic.202200245

Second step: Hydrogen abstraction from $AscOH^-$ and $O_2^{\bullet-}$ reduction

We investigated the substrate reduction to hydroperoxide ion by $AscOH^-$ by exploring the reaction coordinate of hydrogen abstraction from the ascorbate hydroxyl group to the outer oxygen atom of the $O_2^{\bullet-}$. The process is resumed on top of Figure 2. We consider as a starting point the Cu(II)·Aβ·$O_2^{\bullet-}$·$AscOH^-$ isomer in which the hydrogen atom of the OH group on the ascorbate forms an H-bonding interaction with the outer oxygen atom of the $O_2^{\bullet-}$. During this process a concerted e^-/H^+ transfer occurs from the O–H bonding MO of the $AscOH^-$ to the $O_2^{\bullet-}$ with a concomitant formation of a new O–H bonding MO localized on the hydroperoxide.

The reaction free energy of this process is computed using the following equation:

$$\begin{aligned} &Cu(II)\cdot A\beta\cdot O_2^{\bullet-}\cdot AscOH^- + H_2O \rightleftharpoons \\ &Cu(II)\cdot A\beta\cdot O_2H^-\cdot H_2O + AscO^{\bullet-} \end{aligned} \quad (3)$$

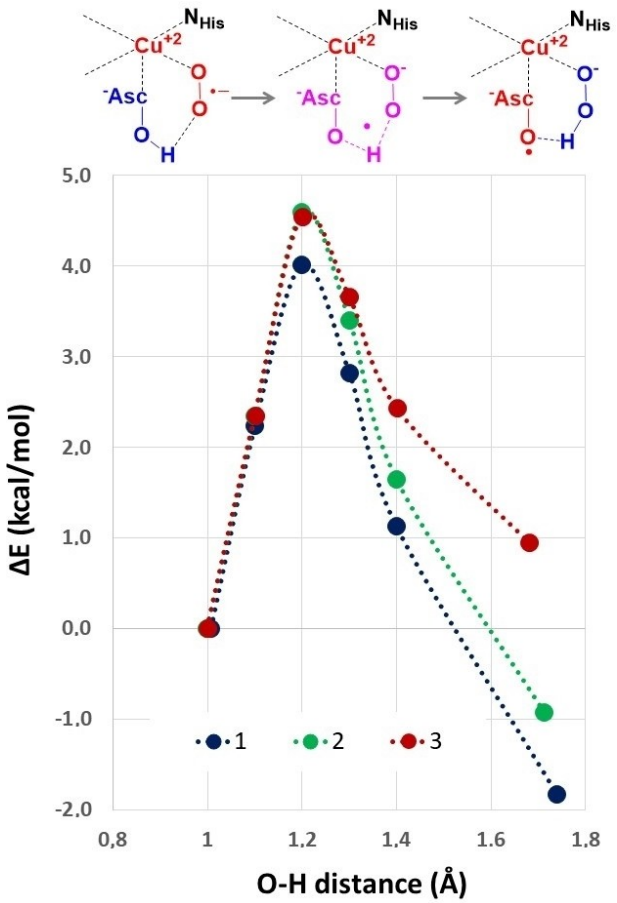

Figure 2. Potential energy surface scans along the hydrogen atom abstraction coordinate of $O_2^{\bullet-}$ reduction to O_2H^- by ascorbate, bound to Cu(II)·Aβ as sketched on top for models **1–3**. In the plot are reported the computed energy differences (in kcal/mol) along the pathway described by the O–H internuclear distance (in Å) between the hydrogen that belongs to the ascorbate hydroxyl group and the outer oxygen atom that belongs to $O_2^{\bullet-}$. On average the computed free energy barrier is 2.7 kcal/mol.

where the geometry and the electronic structure of the Cu(II)·Aβ·O_2H^-·H_2O product will be discussed in the next paragraph.

In Figure 2 the scans along the H abstraction coordinated for the three ascorbate adducts of models **1–3** are reported. The computed free energy barriers are low and equal to 2.7 kcal/mol on average, with a transition state structure slightly closer to the initial reactant with the O–H bond of the hydroxyl group of $AscOH^-$ stretched at 1.2 Å.

At the end of this pathway, we observe the formation of the Cu(II)·Aβ·O_2H^-·$AscO^{\bullet-}$ coordination. According to spin charges, the unpaired electrons are localized on Cu(II) (0.56 e on average that correspond to an Cu 1.7 state), and on the ascorbyl radical (on average 0.98 e), while on the hydroperoxide the initial spin charge of 1.41 is decreased to 0.33 e.

The free energy differences computed according to equation (3) are slightly negative going from −2.4 to −6.6 kcal/mol and on average -5.0 ± 2.3 kcal/mol. Considering this latter average value, the corresponding cell potential

$$\begin{aligned} &E^\circ cell = E^\circ(Cu(II)\cdot A\beta\cdot O_2^{\bullet-}/Cu(II)\cdot A\beta\cdot O_2H^-) \\ &+E^\circ(AscOH^-/AscO^{\bullet-}) \end{aligned} \quad (4)$$

is equal to $E^\circ cell = \Delta G/F = 0.22$ V which must be compared with the value of 1.22 V obtained from the standard reduction potential of O_2^- (0.94 V) and $AscO^{\bullet-}$ (0.28 V). This difference of 1 V is mainly due to the decrease of the oxidative power of the superoxide when coordinated to Cu(II), as also observed in the case of the $OH^\bullet$ radical coordinated to Cu(II) compared to the free solvated $OH^\bullet$ radical. To give a more quantitative estimate of this, we evaluate the decreasing of the O_2^- radical standard reduction potential in Cu(II)·Aβ·O_2^- model coordinations compared to solvated O_2^- (see SI Figure S2 for details). We compute the relative reduction potential $\Delta E^\circ = E^\circ(2)\text{-}E^\circ(1)$ for the following half reactions:

$$\begin{aligned} &Cu(II)\cdot A\beta\cdot O_2^{\bullet-} + e + 2H^+ \rightleftharpoons \\ &Cu(II)\cdot A\beta\cdot O_2H_2\ E^\circ(1) \end{aligned} \quad (1)$$

$$O_2^{\bullet-} + e^- + 2H^+ \rightleftharpoons H_2O_2\ E^\circ(2) \quad (5)$$

where ΔE° does not depend on the potential value of the reference electrode. Recalling that E° of the $O_2^{\bullet-}/H_2O_2$ half-reaction is 0.940 V vs SHE, the E° value for Cu(II)·Aβ·$O_2^{\bullet-}$/Cu(II)·Aβ·O_2H_2 obtained as

$$E^\circ = 0.940\text{-}\Delta E^\circ \quad (6)$$

is −0.06 V, −0.19 V and −0.11 V for **1–3**, respectively.

Stability of the Cu(II)·Aβ·O_2H^- and Cu(II)·Aβ·H_2O_2 coordination modes

Upon e^-/H^+ transfer we observe the formation of the Cu(II)·Aβ·O_2H^-·$AscO^{\bullet-}$ species which eventually undergoes $AscO^{\bullet-}$ detachment with the formation of the Cu(II)·Aβ·O_2H^-

Research Article
doi.org/10.1002/ejic.202200245

species. We describe this latter process according to the following equation:

$$\begin{aligned} &Cu(II)\cdot A\beta\cdot O_2H^-\cdot AscO^{\bullet-}+H_2O\rightleftharpoons\\ &Cu(II)\cdot A\beta\cdot O_2H^-\cdot H_2O+AscO^{\bullet-}\end{aligned} \quad (7)$$

The ligand exchange between the $AscO^{\bullet-}$ radical and the water ligand is energetically favored with a free energy difference equal to −3.5 kcal/mol on average.

$Cu(II)\cdot A\beta\cdot O_2H^-$ has a doublet ground state with an average spin charge on copper equal to 0.56 e that corresponds to a Cu 1.7 redox state, while on the hydroperoxide is 0.29 e. The copper coordination is close to planarity with an O–O bond distance in the hydroperoxide equal to 1.462 Å on average. This analysis is also valid for $Cu(II)\cdot A\beta\cdot H_2O_2$, with the difference that on average the spin population on H_2O_2 is only 0.1 e.

Protonation state of the peroxide product: O_2H^- or H_2O_2?

H_2O_2 is a weak acid with $pK_a = 11.7$ and O_2H^- can be considered a medium/strong base but, when coordinated to Cu(II), O_2H^- basicity is drastically reduced due to its stabilization as a ligand of Cu(II). However, it is important to investigate the stability of the O_2H^- vs H_2O_2 in order to figure out which are the conditions that eventually favor the H_2O_2 release from the metal center, since H_2O_2 is also a neurotoxic reactive oxygen species.[17] By reasoning on the $Cu(II)\cdot A\beta\cdot O_2H^-$ systems, we identify two possible sources of protons, i.e a protonated histidine side chain and protonated Asp or Glu side chain. The possible mechanism for H_2O_2 release could be the following

$$\begin{aligned} &Cu(II)\cdot A\beta\cdot O_2H^-+ResH^+\rightleftharpoons\\ &Cu(II)\cdot A\beta\cdot O_2H_2\cdot Res\rightleftharpoons\\ &Cu(II)\cdot A\beta\cdot Res+H_2O_2\end{aligned} \quad (8)$$

Upon O_2H^- protonation by the protonated residue side chains ($ResH^+$), the resulting labile ligand H_2O_2 is substituted with the de-protonated side chain. Compatible with the possible pH fluctuation on the neuron extracellular environment only histidine (side chain pKa equal to 6.0) could have its protonated state populated in a non-negligible way.

For this reason, we consider the process as described in Figure 3:

- the adduct of the $Cu(II)\cdot A\beta\cdot O_2H^-$ species with a protonated histidine side chain as starting point;
- the transition state of the concerted pathway in which the proton transfer from the protonated imidazole ring in transferred to O_2H^- with the concomitant formation of a new Cu(II)-imidazole bonding interaction;
- the five coordinated $Cu(II)\cdot A\beta\cdot Im\cdot H_2O_2$ adduct in which the deprotonated imidazole ring is bound to Cu(II);
- the dissociation of H_2O_2 form obtaining a four-coordinated $Cu(II)\cdot A\beta$ model.

On average, $Cu(II)\cdot A\beta\cdot ImH^+\cdot O_2H^-$ and $Cu(II)\cdot A\beta\cdot Im\cdot H_2O_2$ species are isoenergetic and the process is characterized by a moderate free energy barrier of 14.9 kcal/mol. Clearly once $Cu(II)\cdot A\beta\cdot H_2O_2$ is formed, H_2O_2 can be easily released (see SI, Figure S2d). These results suggest that H_2O_2 can be moderately released by $Cu(II)\cdot A\beta$ in presence of O_2 and ascorbate, in line with the experimental findings.[75]

H_2O_2 reduction revisited

In a previous investigation on the H_2O_2 reduction that we carried out in our laboratory,[49] we evaluated the barrier for $OH^\bullet$ generation adopting $Cu(I)\cdot A\beta\cdot H_2O_2$ as model coordinations. However, in the computations presented here we explicitly consider the presence of the $AscOH^-$ reductant and, more importantly, the results for the superoxide reduction step clearly suggest that the final product is the hydroperoxide ion instead of H_2O_2. In this section we revisited the $OH^\bullet$ generation by $Cu(II)\cdot A\beta$ in light of these findings by considering the reduction of O_2H^- of the $Cu(II)\cdot A\beta\cdot O_2H^-\cdot AscOH^-$ adducts.

The $Cu(II)\cdot A\beta\cdot O_2H^-\cdot AscOH^-$ adduct has a doublet ground state with spin population localized on the Cu(II), while the corresponding S = 3/2 state is almost 60 kcal/mol higher in energy. Its optimized geometry is similar to that of the corresponding $O_2^{\bullet-}$ adduct, with the hydrogen atom of the OH^- group of the ascorbate that forms an H-bonding interaction with the inner oxygen atom of the O_2H^-. Here the coordination type 3 (with the bound Asp1 amino terminal) is more stable than type 2 (with the bound Asp1 carboxylate side chain) by 9.5 kcal/mol. We describe the hydroperoxide reduction using the following equation:

$$\begin{aligned} &Cu(II)\cdot A\beta\cdot O_2H^-\cdot AscOH^-\rightleftharpoons\\ &Cu(II)\cdot A\beta\cdot (O_2H_2)^-\cdot AscO^{\bullet-}\end{aligned} \quad (9)$$

in which the reduction coordinate is the approaching of the hydrogen atom that belongs to the OH group of $AscOH^-$ with the oxygen atom of the O_2H^- bound to copper.

For the three coordinations considered an average free energy barrier of 2.3 kcal/mol is found at the crossing between the S = 1/2 and S = 3/2 PES. The S = 1/2 broken-symmetry PES solution is very close in energy to S = 3/2 one. The common mechanism observed is reported in Scheme 3A.

At the end of the reaction coordinate, the S = 3/2 structure is characterized by

1. a considerable elongation of the O–O bond (2.268 Å on average);
2. one spin localized on the partially detached $AscO^{\bullet-}$ radical and one on the Cu(II);
3. the two OH ligands sharing one unpaired spin.

These results are in favor of a $Cu(II)\cdot A\beta\cdot (OH)_2^{\bullet-}\cdot AscO^{\bullet-}$ electronic structure. Successively the detach of the ascorbyl radical is largely favored on average by 23.8 kcal/mol with respect to the $Cu(II)\cdot A\beta\cdot O_2H^-\cdot AscOH$ form. Surprisingly, in this last step we observe that OH ligands are able to deprotonate NH_2 amino terminal of Asp1 with the formation of a water molecule that leaves the metal coordination sphere. The

Research Article
doi.org/10.1002/ejic.202200245

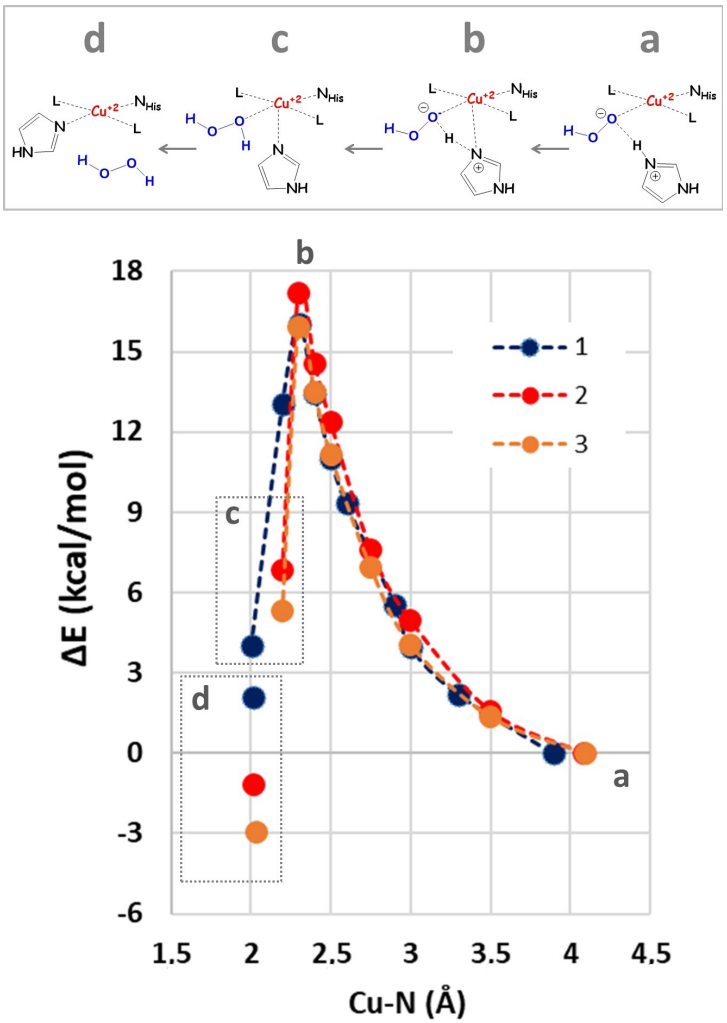

Figure 3. Energy scans (in kcal/mol) along the coordinate describing O_2H^- protonation by protonated His side chain in Cu(II)·Aβ·O_2H^- coordination models **1**–**3** and H_2O_2 release. The energies are reported as a function of the Cu-N_{His} distances (in Å) with the nitrogen atom of the incoming protonated His side chain.

resulting structure is a singlet 5- or 4- coordinated Cu(II) form with one bound OH group.

To further investigate this point, we explored the possible Cu(II) coordination according to Scheme 3B. Beside the Cu-(II)·Aβ·$(OH)_2^{\bullet-}$ form in which one spin is delocalized on two OH ligands (or, alternatively, on a $H_2O_2^-$ moiety η^2-coordinated to copper) one can have i) the Cu(II)·Aβ·$(O^{\bullet-})(H_2O)$ oxyl coordination and ii) the amino deprotonated form. Surprisingly, the most stable η^2-coordinated and NH^- forms sketched below

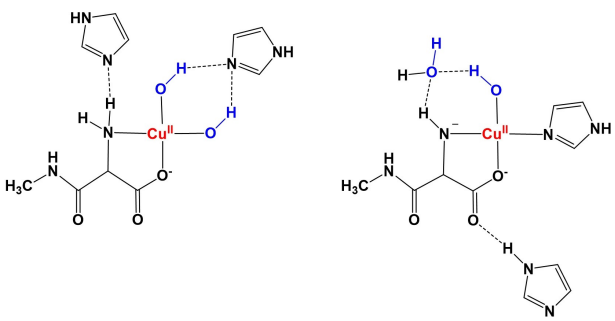

are almost isoenergetic, while the most stable oxyl form is almost 20 kcal/mol higher in energy. As one could expect from simple electrostatic considerations, we observe in the O_2H^- reduction coordinate PES scan that NH^- forms are stabilized when the amino terminal is coordinated to Cu(II) form. By inspecting the their atomic populations (see Figure S4A and B, SI) we observe that half radical character is localized on NH^- thus suggesting that the following process

$$\begin{aligned} &Cu(II)\cdot(NH_2)\cdot A\beta\cdot(OH)_2^{\bullet-} \rightleftharpoons \\ &Cu(II)\cdot[(NH)(OH)]^{\bullet-}\cdot A\beta\cdot(H_2O) \end{aligned} \quad (10)$$

in which the OH radical partially propagates toward terminal NH_2 forming a $NH^{-\bullet}$ radical[76] as sketched below

Research Article
doi.org/10.1002/ejic.202200245

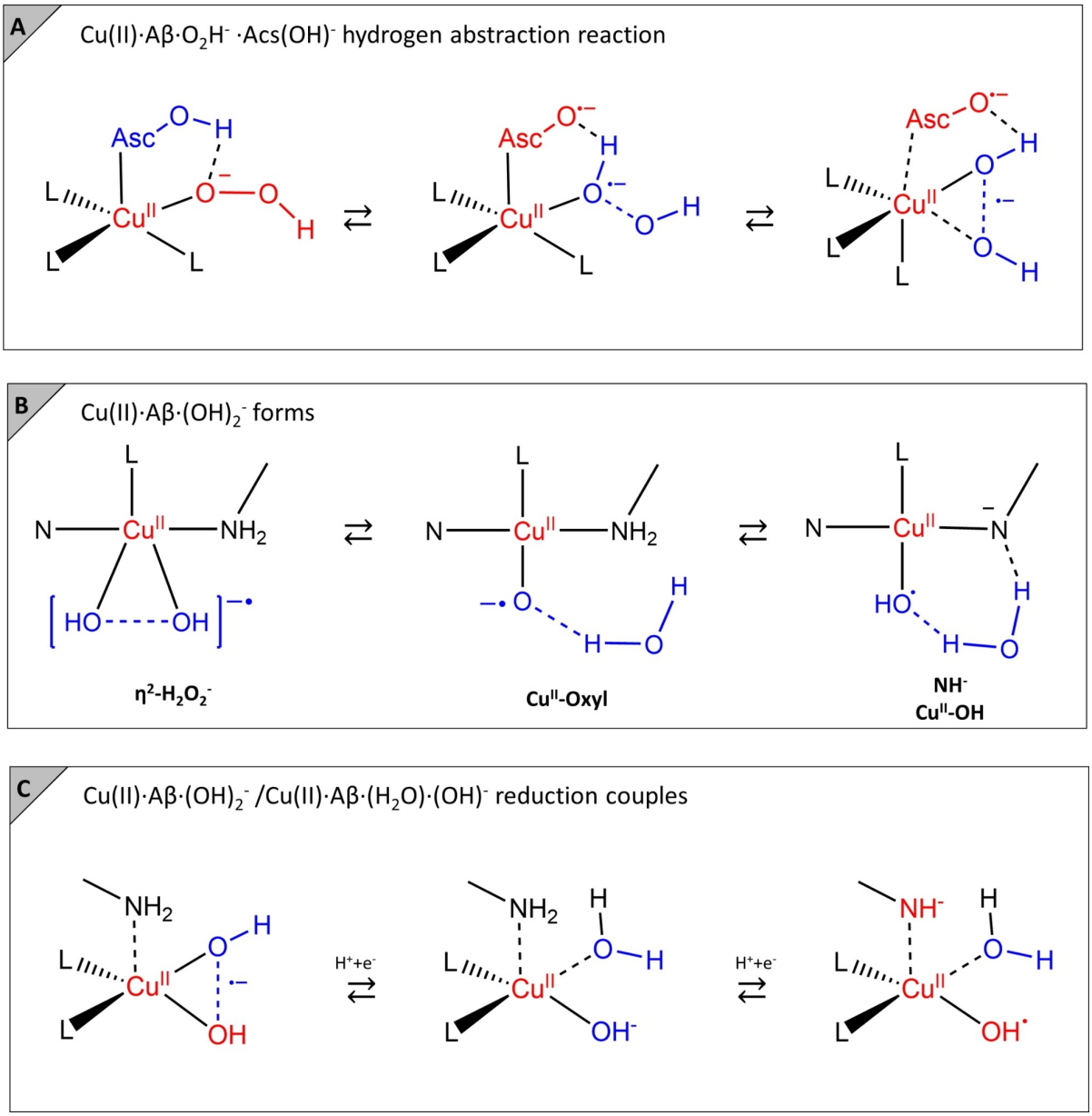

Scheme 3. (A) Hydrogen abstraction reaction of Cu(II)·Aβ·O_2H^-·AcsOH; (B) the three possible Cu(II) coordinations in Cu(II)·Aβ·$(OH)_2^{\bullet-}$; (C) Cu(II)$(OH)_2^-$/ Cu·Aβ·$(H_2O)(OH)^-$ Reduction half-reactions in which both Cu(II)·Aβ·$(OH)_2^-$ isomers are reduced to the same Cu·Aβ·$(H_2O)(OH)^-$ form.

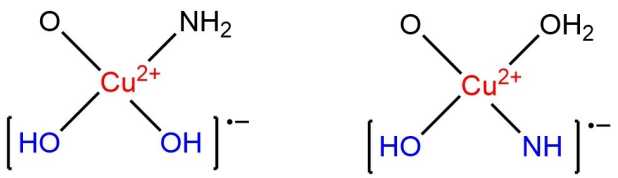

recalling that OH radical is a stronger oxidant than NH_2 radical.[77] We further considered the same models in which 10 explicit water molecules that solvate the OH and NH_2, NH groups are added. At this level the NH form is the most stable while Cu(II)·Aβ·$(OH)_2^{\bullet-}$ form results 5 kcal/mol higher in energy (see Figure S4C, SI).

To establish with more certainty the relative stability of the two coordinations we investigate the NH forms starting from the Cu(II)$(OH)_2^{\bullet-}$·Aβ(1-6) DFT conformational space exploration (Aβ(1-6) is DAEFRH C-terminus capped peptide; see SI for details) previously carried out in our laboratory.[20]

We observe that lower energy forms are mostly four-coordinated and that the most stable Cu(II)Aβ(1-6)$(OH)_2^{\bullet-}$ coordination is 6.1 kcal/mol higher in energy compared to the corresponding most stable NH form (Figure 4). In the latter, the His6 side chain replaces the leaving water molecules from the Cu(II) coordination sphere, suggesting that the formation of the deprotonated form is favored either by entropic or enthalpic effects.

Research Article
doi.org/10.1002/ejic.202200245

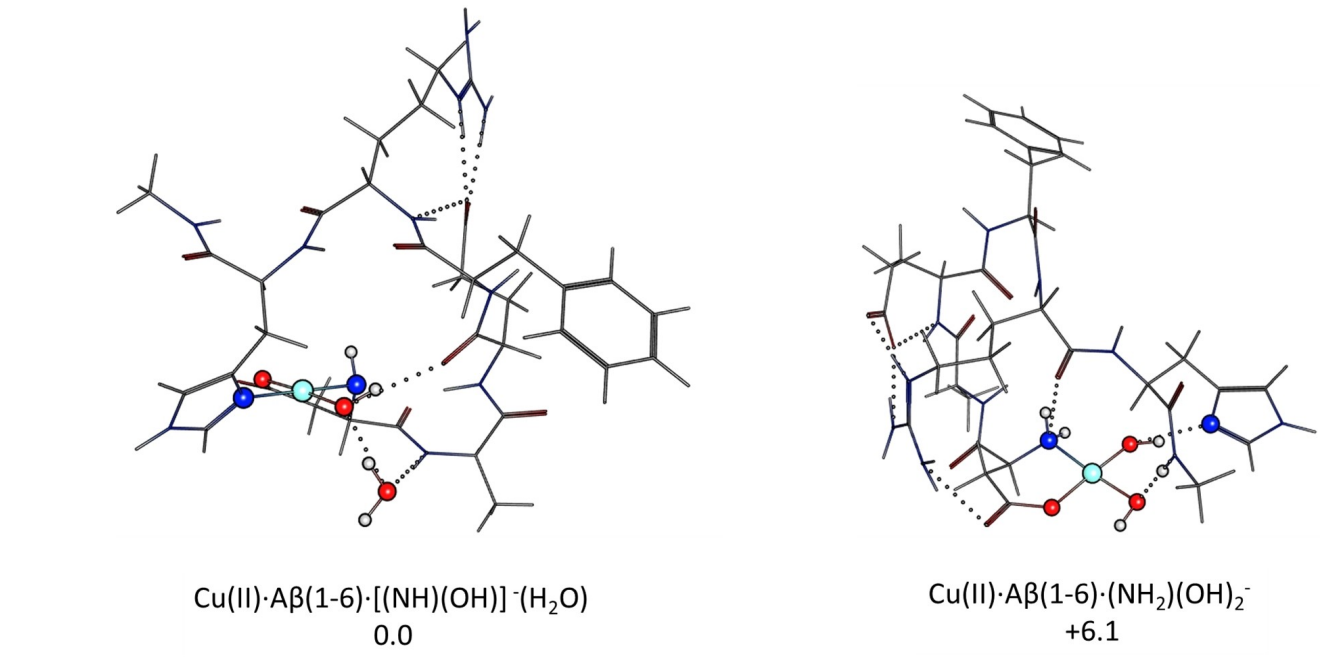

Figure 4. Sketches of the Cu(II)·Aβ(1-6)·$(NH_2)(OH)_2^{\bullet -}$ form and the NH^- terminal Cu(II)·Aβ(1-6)·$[(NH)(OH)]^{-\bullet}(H_2O)$ lowest energy structure (Aβ(1-6) DAEFRH C-terminus capped peptide). Dotted lines underline Hydrogen bond interactions and salt-bridge interactions that involve Arg5 side chain. The computed total energy difference is in kcal/mol.

Gathering all the evidence regarding this point *we suggest that the formation of the NH form is an OH propagation intramolecular step* and we estimated that its standard reduction potential is less oxidant by 0.13 V compared to the corresponding Cu(II)·Aβ·$(OH)_2^{\bullet -}$. Moreover, in the oxidative damage of Aβ induced by Cu(II)·Aβ·OH N-terminus is a privileged[78] site and therefore this NH radical form could be involved in this process.

Discussion and conclusion

From the data proposed above and summarized in Figure 5 for the three Cu(II)·Aβ·$O_2^{\bullet -}$ (**1**–**3**) coordinations, the picture emerged from DFT computations is that the $O_2^{\bullet -} \rightarrow O_2H^-$ and $O_2H^- \rightarrow (OH)_2^{\bullet -}$ reductions catalyzed by Cu(II)·Aβ with ascorbate as reducing agents are thermodynamically and kinetically favorable.

Resuming for the reaction steps leading to the final Cu(II)·Aβ·O_2H^- reduction we observe that

1. Ascorbate affinity to Cu(II)·Aβ·$O_2^{\bullet -}$ or Cu(II)·Aβ·O_2H^- is low with a positive binding free energy on average of 2.7 and 5.3 kcal/mol, respectively;
2. the hydrogen atom abstraction from ascorbate (see equation 3 and equation 9 above) in Cu(II)·Aβ·$O_2^{\bullet -}$·$AscOH^-$ and Cu(II)·Aβ·O_2H^-·$AscOH^-$ have free energy barriers of 2.0 and 2.3 kcal/mol, respectively;
3. the reaction free energy of the Cu(II)·Aβ·$O_2^{\bullet -}$ reduction is on average −0.3 kcal/mol, while Cu(II)·Aβ·O_2H^- reduction is highly exergonic on average by −21.5 kcal/mol;
4. the most stable final product Cu(II)·Aβ·$(OH)_2^{\bullet -}$ has a N-amino terminal Asp1 radical.

Since these results have been obtained using the same level of theory and the same approach adopted in our previous investigation on O_2 activation and reduction, we can discuss the free energy difference values computed for the whole process of OH radical formation. Along the OH• production catalyzed by Cu(II)·Aβ, these investigations highlights that:

1. the rate determining step of the OH production is the O_2 binding to Cu(I);
2. the product of $O_2^{\bullet -}$ reduction is Cu(II) coordinated O_2H^- hydroperoxide anion and not H_2O_2;
3. $O_2^{\bullet -}$ can dissociate from Cu(II)·Aβ first coordination as well as H_2O_2, although with a lesser extent;
4. the three intermediates of OH• production ($O_2^{\bullet -}$, O_2H^- and OH• radical coordinated to Cu(II)·Aβ) are less redox active compared to the corresponding form in solution, according to the estimated reduction potentials due to the Cu(II) binding.

The emerging evidence here is that once monomeric or small oligomers soluble Aβ peptide systems bind Cu(II), the high physiological concentration of molecular oxygen and ascorbate in the brain can favor OH production, whose only relevant activation barrier is that of oxygen binding to reduced Cu(I)·Aβ. Once Cu(I)·Aβ·O_2 is formed, the production of OH radical thought Fenton-like mechanism in presence of ascorbate is characterized by low free energy barriers and therefore is almost inevitable and the final Cu(II)·Aβ·OH• ROS we identified can induce oxidative stress. In view of the antioxidant therapy, this final species could be the pharmacological target.

Research Article
doi.org/10.1002/ejic.202200245

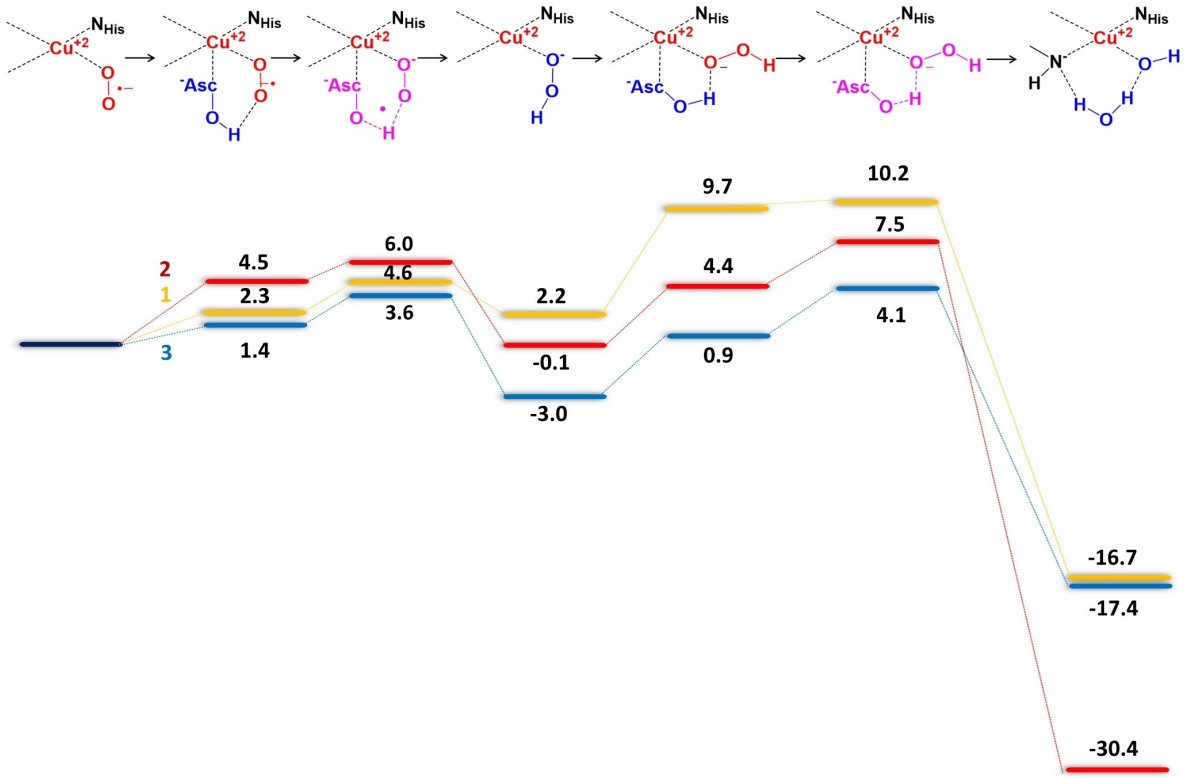

Figure 5. Schematic representation of the mechanism O_2^- reduction to hydroperoxide and then to hydroxyl radical plus OH^- catalyzed by Cu(II)·Aβ in presence of $AscOH^-$ ascorbate as one-electron reductant. Free energies differences (kcal/mol) are computed with respect to Cu(II)·Aβ·$O_2^{\bullet-}$ **1**–**3** forms.

We observe that Cu(II)·Aβ is a $O_2^{\bullet-}$ producer and that $O_2^{\bullet-}$ can leave the Cu(II) coordinations sphere if it is stabilized by non-bonding interactions, in line with the finding of Reybier et al.[50] confirming the possibility that superoxide also can contribute to oxidative stress in AD. The same holds true for H_2O_2 but with a much lesser extent due to the 14.9 kcal/mol free energy barrier for H_2O_2 dissociation.

The fact that Cu(II)[(NH)(OH)]$^{\bullet}$·Aβ(1-6) is more stable (on average by 5.8 kcal/mol see SI) than Cu(II)·$(OH)_2^{\bullet-}$Aβ(1-6) form could have a role in mechanism of $OH^{\bullet}$ propagation that induces oxidative stress in AD. When $OH^{\bullet}$ radical propagates, the final product is always Cu(II)·$(NH_2)(H_2O)(OH)^-$ (see Scheme 3C); since NH radical form is more stable, this implies that this form is also less oxidizing (roughly 0.13 V) and therefore the $OH^{\bullet}$ will have an even longer lifetime to diffuse into the cell membrane lipid bilayer, starting lipid peroxidation.

In conclusion, this detailed study completes the DFT picture of the Fenton-like O_2 reduction catalyzed by Aβ peptide in presence of ascorbate and suggest the structure of the the most likely Cu(II)·Aβ·$OH^{\bullet}$ coordinations responsible for $OH^{\bullet}$ production, and thus oxidative stress in AD. Finally, our results clearly demonstrate, once again, the relevance of *ab initio* DFT modelling from basic \research to the development of therapeutic strategies in AD.

Acknowledgements

Open Access Funding provided by Università degli studi di Milano-Bicocca within the CRUI-CARE Agreement. Open Access Funding provided by Universita degli Studi di Milano-Bicocca within the CRUI-CARE Agreement.

Conflict of Interest

The authors declare no conflict of interest.

Data Availability Statement

The data that support the findings of this study are available in the supplementary material of this article.

Keywords: Alzheimer's disease · Copper · Density functional theory calculations · Metal dyshomeostasis · Oxidative stress · Reactive oxygen species

[1] C. Ballard, S. Gauthier, A. Corbett, C. Brayne, D. Aarsland, E. Jones, *The Lancet* **2011**, *377*, 1019–1031.
[2] D. S. Knopman, H. Amieva, R. C. Petersen, G. Chételat, D. M. Holtzman, B. T. Hyman, R. A. Nixon, D. T. Jones, *Nat Rev Dis Primers* **2021**, *7*, 33.

[3] G. B. Frisoni, D. Altomare, D. R. Thal, F. Ribaldi, R. van der Kant, R. Ossenkoppele, K. Blennow, J. Cummings, C. van Duijn, P. M. Nilsson, P.-Y. Dietrich, P. Scheltens, B. Dubois, *Nat. Rev. Neurosci.* **2022**, *23*, 53–66.
[4] GBD 2019 Dementia Forecasting Collaborators, *Lancet Public Health* **2022**, DOI 10.1016/S2468-2667(21)00249–8.
[5] J. Hardy, G. Higgins, *Science* **1992**, *256*, 184–185.
[6] J. Hardy, *Journal of Alzheimer's Disease* **2006**, *9*, 151–153.
[7] E. Karran, M. Mercken, B. De Strooper, *Nat. Rev. Drug Discovery* **2011**, *10*, 698–712.
[8] M. Rana, A. K. Sharma, *Metallomics* **2019**, *11*, 64–84.
[9] M. Tolar, J. Hey, A. Power, S. Abushakra, *Int. J. Mol. Sci.* **2021**, *22*, 6355.
[10] A. Rauk, *Chem. Soc. Rev.* **2009**, *38*, 2698–2715.
[11] S. Bagheri, R. Squitti, T. Haertlé, M. Siotto, A. A. Saboury, *Front. Aging Neurosci.* **2017**, *9*, 446.
[12] G. Eskici, P. H. Axelsen, *Biochemistry* **2012**, *51*, 6289–6311.
[13] M. A. Greenough, J. Camakaris, A. I. Bush, *Neurochem. Int.* **2013**, *62*, 540–555.
[14] E. Atrián-Blasco, P. Gonzalez, A. Santoro, B. Alies, P. Faller, C. Hureau, *Coord. Chem. Rev.* **2018**, *371*, 38–55.
[15] C. Cheignon, M. Tomas, D. Bonnefont-Rousselot, P. Faller, C. Hureau, F. Collin, *Redox Biology* **2018**, *14*, 450–464.
[16] K. P. Kepp, R. Squitti, *Coord. Chem. Rev.* **2019**, *397*, 168–187.
[17] X. Huang, M. P. Cuajungco, C. S. Atwood, M. A. Hartshorn, J. D. A. Tyndall, G. R. Hanson, K. C. Stokes, M. Leopold, G. Multhaup, L. E. Goldstein, R. C. Scarpa, A. J. Saunders, J. Lim, R. D. Moir, C. Glabe, E. F. Bowden, C. L. Masters, D. P. Fairlie, R. E. Tanzi, A. I. Bush, *J. Biol. Chem.* **1999**, *274*, 37111–37116.
[18] D. A. Butterfield, D. Boyd-Kimball, *J. Neurochem.* **2019**, *151*, 459–487.
[19] C. Cheignon, C. Hureau, F. Collin, *Inorg. Chim. Acta* **2018**, *472*, 111–118.
[20] F. Arrigoni, F. Rizza, R. Tisi, L. De Gioia, G. Zampella, L. Bertini, *Metallomics* **2020**, *12*, 1765–1780.
[21] B. Halliwell, J. M. C. Gutteridge, *J. Free Radicals Biol. Med.* **1985**, *1*, 331–332.
[22] D. A. Butterfield, *Ageing Res. Rev.* **2020**, 101049.
[23] S. K. T. S. Wärmländer, N. Österlund, C. Wallin, J. Wu, J. Luo, A. Tiiman, J. Jarvet, A. Gräslund, *J. Biol. Inorg. Chem.* **2019**, *24*, 1189–1196.
[24] F. Collin, *Int. J. Mol. Sci.* **2019**, *20*, DOI 10.3390/ijms20102407.
[25] R. Squitti, P. Faller, C. Hureau, A. Granzotto, A. R. White, K. P. Kepp, *Journal of Alzheimer's Disease* **2021**, *83*, 23–41.
[26] C. Cheignon, M. Jones, E. Atrián-Blasco, I. Kieffer, P. Faller, F. Collin, C. Hureau, *Chem. Sci.* **2017**, *8*, 5107–5118.
[27] C. S. Atwood, R. C. Scarpa, X. Huang, R. D. Moir, W. D. Jones, D. P. Fairlie, R. E. Tanzi, A. I. Bush, *J. Neurochem.* **2000**, *75*, 1219–1233.
[28] P. Faller, C. Hureau, *Dalton Trans.* **2009**, 1080–1094.
[29] P. Faller, C. Hureau, O. Berthoumieu, *Inorg. Chem.* **2013**, *52*, 12193–12206.
[30] B. J. Tabner, J. Mayes, D. Allsop, *Int. J. Alzheimers. Dis.* **2010**, *2011*, 546380.
[31] M. A. Lovell, J. D. Robertson, W. J. Teesdale, J. L. Campbell, W. R. Markesbery, *J. Neurol. Sci.* **1998**, *158*, 47–52.
[32] L. M. Miller, Q. Wang, T. P. Telivala, R. J. Smith, A. Lanzirotti, J. Miklossy, *J. Struct. Biol.* **2006**, *155*, 30–37.
[33] S. A. James, Q. I. Churches, M. D. de Jonge, I. E. Birchall, V. Streltsov, G. McColl, P. A. Adlard, D. J. Hare, *ACS Chem. Neurosci.* **2017**, *8*, 629–637.
[34] L. M. Sayre, D. A. Zelasko, P. L. Harris, G. Perry, R. G. Salomon, M. A. Smith, *J. Neurochem.* **1997**, *68*, 2092–2097.
[35] Y. H. Hung, A. I. Bush, R. A. Cherny, *J. Biol. Inorg. Chem.* **2010**, *15*, 61–76.
[36] D. Strozyk, L. J. Launer, P. A. Adlard, R. A. Cherny, A. Tsatsanis, I. Volitakis, K. Blennow, H. Petrovitch, L. R. White, A. I. Bush, *Neurobiol. Aging* **2009**, *30*, 1069–1077.
[37] S. Bucossi, M. Ventriglia, V. Panetta, C. Salustri, P. Pasqualetti, S. Mariani, M. Siotto, P. M. Rossini, R. Squitti, *Journal of Alzheimer's Disease* **2011**, *24*, 175–185.
[38] E. Atrián-Blasco, M. Del Barrio, P. Faller, C. Hureau, *Anal. Chem.* **2018**, *90*, 5909–5915.
[39] V. Balland, C. Hureau, J.-M. Saveant, *Proc. Natl. Acad. Sci. USA* **2010**, *107*, 17113–17118.
[40] F. Arrigoni, T. Prosdocimi, L. Mollica, L. De Gioia, G. Zampella, L. Bertini, *Metallomics* **2018**, *10*, 1618–1630.
[41] M. E. Rice, *Trends Neurosci.* **2000**, *23*, 209–216.
[42] S. C. Drew, K. J. Barnham, *Acc. Chem. Res.* **2011**, *44*, 1146–1155.
[43] L. G. Trujano-Ortiz, F. J. González, L. Quintanar, *Inorg. Chem.* **2015**, *54*, 4–6.
[44] B. Alies, H. Eury, C. Bijani, L. Rechignat, P. Faller, C. Hureau, *Inorg. Chem.* **2011**, *50*, 11192–11201.
[45] J. Alí-Torres, J.-D. Maréchal, L. Rodríguez-Santiago, M. Sodupe, *J. Am. Chem. Soc.* **2011**, *133*, 15008–15014.
[46] S. Furlan, C. Hureau, P. Faller, G. La Penna, *J. Phys. Chem. B* **2012**, *116*, 11899–11910.
[47] A. Mirats, J. Alí-Torres, L. Rodríguez-Santiago, M. Sodupe, G. La Penna, *Phys. Chem. Chem. Phys.* **2015**, *17*, 27270–27274.
[48] S. Furlan, C. Hureau, P. Faller, G. La Penna, *J. Phys. Chem. B* **2010**, *114*, 15119–15133.
[49] T. Prosdocimi, L. De Gioia, G. Zampella, L. Bertini, *J. Biol. Inorg. Chem.* **2016**, *21*, 197–212.
[50] K. Reybier, S. Ayala, B. Alies, J. V. Rodrigues, S. B. Rodriguez, G. La Penna, F. Collin, C. M. Gomes, C. Hureau, P. Faller, *Angew. Chem.* **2016**, *128*, 1097–1101; *Angew. Chem. Int. Ed.* **2016**, *55*, 1085–1089.
[51] T. Persson, B. O. Popescu, A. Cedazo-Minguez, *Oxidative Medicine and Cellular Longevity* **2014**, *2014*, 1–11.
[52] S. C. Drew, *Front. Neurol. Neurosci.* **2017**, *11*, 317.
[53] R. N. Martins, C. S. Brennan, *Neurodegeneration and Alzheimer's Disease: The Role of Diabetes, Genetics, Hormones, and Lifestyle*, John Wiley & Sons, **2019**.
[54] L. E. McInnes, A. Noor, K. Kysenius, C. Cullinane, P. Roselt, C. A. McLean, F. C. K. Chiu, A. K. Powell, P. J. Crouch, J. M. White, P. S. Donnelly, *Inorg. Chem.* **2019**, *58*, 3382–3395.
[55] S. K. A. Opare, A. Rauk, *J. Phys. Chem. B* **2017**, *121*, 11304–11310.
[56] Y. Wang, T. T. Huynh, H.-J. Cho, Y.-C. Wang, B. E. Rogers, L. M. Mirica, *Inorg. Chem.* **2021**, *60*, 12610–12620.
[57] E. Atrián-Blasco, E. Cerrada, A. Conte-Daban, D. Testemale, P. Faller, M. Laguna, C. Hureau, *Metallomics* **2015**, *7*, 1229–1232.
[58] D. Chaparro, A. Flores-Gaspar, J. Alí-Torres, *J. Alzheimer's Dis.* **2021**, *82*, S179–S193.
[59] G. La Penna, C. Hureau, O. Andreussi, P. Faller, *J. Phys. Chem. B* **2013**, *117*, 16455–16467.
[60] J. Nasica-Labouze, P. H. Nguyen, F. Sterpone, O. Berthoumieu, N.-V. Buchete, S. Coté, A. De Simone, A. J. Doig, P. Faller, A. Garcia, A. Laio, M. S. Li, S. Melchionna, N. Mousseau, Y. Mu, A. Paravastu, S. Pasquali, D. J. Rosenman, B. Strodel, B. Tarus, J. H. Viles, T. Zhang, C. Wang, P. Derreumaux, *Chem. Rev.* **2015**, *115*, 3518–3563.
[61] B. Strodel, O. Coskuner-Weber, *J. Chem. Inf. Model.* **2019**, *59*, 1782–1805.
[62] N. Hewitt, A. Rauk, *J. Phys. Chem. B* **2009**, *113*, 1202–1209.
[63] R. Giacovazzi, I. Ciofini, L. Rao, C. Amatore, C. Adamo, *Phys. Chem. Chem. Phys.* **2014**, *16*, 10169–10174.
[64] A. D. Becke, *Phys. Rev. A Gen. Phys.* **1988**, *38*, 3098–3100.
[65] J. P. Perdew, *Phys. Rev. B Condens. Matter* **1986**, *33*, 8822–8824.
[66] K. Eichkorn, F. Weigend, O. Treutler, R. Ahlrichs, *Theor. Chem. Acc.* **1997**, *97*, 119–124.
[67] R. Ahlrichs, M. Bär, M. Häser, H. Horn, C. Kölmel, *Chem. Phys. Lett.* **1989**, *162*, 165–169.
[68] A. Schäfer, C. Huber, R. Ahlrichs, *J. Chem. Phys.* **1994**, *100*, 5829–5835.
[69] A. Klamt, G. Schüürmann, *J. Chem. Soc. Perkin Trans. 2* **1993**, 799–805.
[70] L. Bertini, M. Bruschi, M. Romaniello, G. Zampella, M. Tiberti, V. Barbieri, C. Greco, D. La Mendola, R. P. Bonomo, P. Fantucci, L. De Gioia, in *Highlights in Theoretical Chemistry*, **2012**, pp. 255–269.
[71] R. Breglia, F. Arrigoni, M. Sensi, C. Greco, P. Fantucci, L. De Gioia, M. Bruschi, *Inorg. Chem.* **2021**, *60*, 387–402.
[72] D. J. Anick, *J. Phys. Chem. A* **2011**, *115*, 6327–6338.
[73] P. Wu, J. Zhang, Q. Chen, W. Peng, B. Wang, *Chin. J. Catal.* **2022**, *43*, 913–927.
[74] W. D. Bailey, D. Dhar, A. C. Cramblitt, W. B. Tolman, *J. Am. Chem. Soc.* **2019**, *141*, 5470–5480.
[75] B. Alies, I. Sasaki, O. Proux, S. Sayen, E. Guillon, P. Faller, C. Hureau, *Chem. Commun.* **2013**, *49*, 1214.
[76] J. Hioe, D. Šakić, V. Vrček, H. Zipse, *Org. Biomol. Chem.* **2015**, *13*, 157–169.
[77] J. Zhong, Y. Zhao, L. Li, H. Li, J. S. Francisco, X. C. Zeng, *J. Am. Chem. Soc.* **2015**, *137*, 12070–12078.
[78] L.-E. Cassagnes, V. Hervé, F. Nepveu, C. Hureau, P. Faller, F. Collin, *Angew. Chem. Int. Ed. Engl.* **2013**, *52*, 11110–11113.

Manuscript received: April 19, 2022
Revised manuscript received: May 10, 2022
Accepted manuscript online: May 14, 2022